iScience, Volume *27*

Supplemental information

Development and validation of a multimodal deep learning framework for vascular cognitive impairment diagnosis

Fan Fan, Hao Song, Jiu Jiang, Haoying He, Dong Sun, Zhipeng Xu, Sisi Peng, Ran Zhang, Tian Li, Jing Cao, Juan Xu, Xiaoxiang Peng, Ming Lei, Chu He, and Junjian Zhang

Table S1. Performance metrics of the multimodal deep learning model, related to Figure 1.

	Accuracy	Sensitivity	Specificity	F1-score	AUC	AP
sMRI only model						
T1	0.855 [0.774-0.936]	0.936 [0.857-1.000]	0.774 [0.640-0.903]	0.866 [0.787-0.936]	0.905 [0.834-0.963]	0.901 [0.819-0.969]
T2-FLAIR	0.855 [0.774-0.919]	0.903 [0.807-0.972]	0.807 [0.679-0.929]	0.862 [0.774-0.932]	0.861 [0.769-0.938]	0.828 [0.708-0.940]
Clinical non-imaging model						
31 clinical variables	0.855 [0.774-0.919]	0.968 [0.909-1.000]	0.742 [0.600-0.971]	0.870 [0.794-0.936]	0.927 [0.874-0.974]	0.936 [0.886-0.976]
Hybrid model						
Clinical + T1	0.887 [0.823-0.952]	0.903 [0.808-0.971]	0.871 [0.765-0.968]	0.889 [0.813-0.952]	0.965 [0.923-0.993]	0.972 [0.940-0.994]
Clinical + T2	0.855 [0.774-0.936]	0.936 [0.857-1.000]	0.774 [0.650-0.900]	0.866 [0.793-0.933]	0.953 [0.903-0.992]	0.964 [0.926-0.992]
Clinical + T1 + T2	0.919 [0.855-0.968]	0.968 [0.909-1.000]	0.871 [0.765-0.968]	0.923 [0.863-0.972]	0.972 [0.934-0.997]	0.979 [0.951-0.997]

Note: The performance of the sMRI-only model (ViT), the clinical non-imaging model (XGBoost), and the hybrid model (ViT + XGBoost) for the VCI diagnosis are shown through reporting the accuracy, sensitivity, specificity, F1-score, AUC, and AP. All metrics are presented as the mean [95% confidence interval].

Abbreviations: AUC, area under the receiver operating characteristic curve; AP, area under the precision-recall curve; sMRI, structural magnetic resonance imaging; FLAIR, fluid attenuated inversion recovery; ViT, Vision Transformer; XGBoost, extreme gradient boosting.

Table S2. The importance scores of 116 anatomical regions in AAL atlas, related to Figure 4.

Brain regions	Importance score (T1/T2-FLAIR)	Brain regions	Importance score (T1/T2-FLAIR)
Precentral_L	0.130/0.105	Superior parietal_L	0.000/0.123
Precentral_R	0.001/0.007	Superior parietal_R	0.472/0.004
Superior frontal_L	0.005/0.248	Inferior parietal_L	0.032/0.021
Superior frontal_R	0.100/0.143	Inferior parietal_R	0.084/0.022
Superior frontal orbital_L	0.000/0.549	Supramarginal_L	0.000/0.045
Superior frontal orbital_R	0.121/0.490	Supramarginal_R	0.001/0.026
Middle frontal_L	0.005/0.119	Angular_L	0.134/0.045
Middle frontal_R	0.016/0.100	Angular_R	0.176/0.044
Middle frontal orbital_L	0.033/0.706	Precuneus_L	0.022/0.341
Middle frontal orbital_R	0.003/0.129	Precuneus_R	0.008/0.161
Inferior frontal opercular_L	0.430/0.477	Paracentral lobule_L	0.000/0.004
Inferior frontal opercular_R	0.085/0.000	Paracentral lobule_R	0.011/0.000
Inferior frontal triangular_L	0.461/0.592	Caudate_L	0.000/0.054
Inferior frontal triangular_R	0.130/0.003	Caudate_R	0.003/0.017
Inferior frontal orbital_L	0.483/0.651	Putamen_L	0.000/0.003
Inferior frontal orbital_R	0.010/0.002	Putamen_R	0.074/0.289
Rolandic operculum_L	0.035/0.017	Pallidum_L	0.000/0.000
Rolandic operculum_R	0.000/0.000	Pallidum_R	0.000/0.022
Supplementary motor area_L	0.000/0.210	Thalamus_L	0.000/0.000
Supplementary motor area_R	0.006/0.080	Thalamus_R	0.107/0.000
Olfactory_L	0.000/0.249	Heschl_L	0.000/0.000
Olfactory_R	0.000/0.031	Heschl_R	0.002/0.000
Superior medial frontal_L	0.040/0.555	Superior temporal_L	0.001/0.102
Superior medial frontal_R	0.175/0.383	Superior temporal_R	0.049/0.174
Medial frontal orbital_L	0.000/0.752	Superior temporal pole_L	0.426/0.076
Medial frontal orbital_R	0.043/0.976	Superior temporal pole_R	0.130/0.215
Rectus_L	0.000/0.771	Middle temporal_L	0.011/0.122
Rectus_R	0.081/0.599	Middle temporal_R	0.004/0.199
Insula_L	0.107/0.024	Middle temporal pole_L	0.181/0.046
Insula_R	0.025/0.365	Middle temporal pole_R	0.430/0.120
Anterior cingulate_L	0.026/1.000	Inferior temporal_L	0.159/0.033
Anterior cingulate_R	0.356/0.971	Inferior temporal_R	0.007/0.020
Median cingulate_L	0.001/0.106	Cerebelum crus1_L	0.328/0.023
Median cingulate_R	0.224/0.326	Cerebelum crus1_R	0.271/0.131
Posterior cingulate_L	0.000/0.000	Cerebelum crus2_L	0.191/0.015
Posterior cingulate_R	0.002/0.004	Cerebelum crus2_R	0.547/0.332
Hippocampus_L	0.000/0.000	Cerebelum 3_L	0.000/0.000
Hippocampus_R	0.062/0.245	Cerebelum 3_R	1.000/0.000
Parahippocampal_L	0.000/0.000	Cerebelum 4 and 5_L	0.003/0.000
Parahippocampal_R	0.081/0.017	Cerebelum 4 and 5_R	0.453/0.000

Amygdala_L	0.000/0.000	Cerebelum 6_L	0.003/0.000
Amygdala_R	0.008/0.574	Cerebelum 6_R	0.146/0.001
Calcarine_L	0.316/0.001	Cerebelum 7b_L	0.223/0.000
Calcarine_R	0.002/0.000	Cerebelum 7b_R	0.301/0.007
Cuneus_L	0.013/0.487	Cerebelum 8_L	0.146/0.000
Cuneus_R	0.004/0.019	Cerebelum 8_R	0.267/0.000
Lingual_L	0.131/0.000	Cerebelum 9_L	0.422/0.000
Lingual_R	0.078/0.000	Cerebelum 9_R	0.685/0.000
Superior occipital_L	0.048/0.440	Cerebelum 10_L	0.502/0.000
Superior occipital_R	0.011/0.109	Cerebelum 10_R	0.000/0.000
Middle occipital_L	0.325/0.020	Vermis 1 and 2	0.670/0.000
Middle occipital_R	0.043/0.563	Vermis 3	0.574/0.000
Inferior occipital_L	0.045/0.000	Vermis 4 and 5	0.079/0.000
Inferior occipital_R	0.000/0.000	Vermis 6	0.017/0.000
Fusiform_L	0.003/0.006	Vermis 7	0.144/0.000
Fusiform_R	0.014/0.020	Vermis 8	0.040/0.000
Postcentral_L	0.041/0.004	Vermis 9	0.000/0.000
Postcentral_R	0.072/0.081	Vermis 10	0.068/0.000

Note: The contribution of T1 and T2-FLAIR image features to the VCI diagnosis within each brain region was quantified by calculating the importance scores, respectively.

Abbreviations: AAL, anatomical automatic labeling; FLAIR, fluid attenuated inversion recovery; VCI, vascular cognitive impairment.

Table S3. The non-imaging variables and associated data missing rate, related to STAR Methods.

Variables	Model construction cohort (n=307)	Missing data rate, %	External validation cohort (n=157)	Missing data rate, %
Demographics				
Age	307	0.00	157	0.00
Sex	307	0.00	157	0.00
Marital status	305	0.65	155	1.27
Education years	302	1.63	157	0.00
Medical history				
Hypertension	306	0.33	151	3.82
Diabetes	306	0.33	151	3.82
Hyperlipidemia	306	0.33	151	3.82
CHD	306	0.33	143	8.92
TIA	306	0.33	142	9.55
Stroke	244	20.52	143	8.92
Intra/extracranial artery stenosis	306	0.33	153	2.55
Family history				
Family history of stroke	289	5.86	135	14.01
Family history of dementia	289	5.86	137	12.74
Family history of hypertension	289	5.86	135	14.01
Family history of diabetes	289	5.86	139	11.46
Family history of CHD	289	5.86	142	9.55
Medication history				
Antiplatelet	302	1.63	157	0.00
Anticoagulant	227	26.06	143	8.92
Lipid-lowering	302	1.63	152	3.18
Antihypertensive	302	1.63	152	3.18
Anti-dementia	234	23.78	136	13.38
Antidiabetic	300	2.28	153	2.55
Daily habits				
Physical exercise	292	4.89	152	3.18
Dietary habit	167	45.60	111	29.30
Sleeping habit	175	43.00	131	16.56
Smoking	305	0.65	157	0.00
Drinking	305	0.65	153	2.55
Physical measures				
Height	291	5.21	154	1.91
Weight	291	5.21	154	1.91
Body mass index	291	5.21	154	1.91
Systolic blood pressure	293	4.56	155	1.27

Diastolic blood pressure	293	4.56	155	1.27
Laboratory tests				
Leukocyte counts	290	5.54	155	1.27
Erythrocyte counts	292	4.89	155	1.27
Hemoglobin	292	4.89	155	1.27
Platelet counts	292	4.89	155	1.27
Fasting blood glucose	289	5.86	147	6.37
Glycated hemoglobin	148	51.79	120	23.57
Total cholesterol	289	5.86	154	1.91
LDL-C	290	5.54	154	1.91
HDL-C	287	6.51	154	1.91
Triglyceride	287	6.51	154	1.91
Fibrinogen	274	10.75	143	8.92
Alanine aminotransferase	294	4.23	152	3.18
Aspartate aminotransferase	294	4.23	152	3.18
Albumin	294	4.23	152	3.18
Globulin	293	4.56	152	3.18
A/G	293	4.56	152	3.18
Total bilirubin	294	4.23	152	3.18
Direct bilirubin	294	4.23	152	3.18
Indirect bilirubin	294	4.23	152	3.18
Creatinine	292	4.89	152	3.18
Urea nitrogen	291	5.21	152	3.18
Homocysteine	104	66.12	116	26.11

Abbreviations: CHD, coronary heart disease; TIA, transient ischemic attack; LDL-C, low density lipoprotein cholesterol; HDL-C, high density lipoprotein cholesterol; A/G, albumin-globulin ratio.

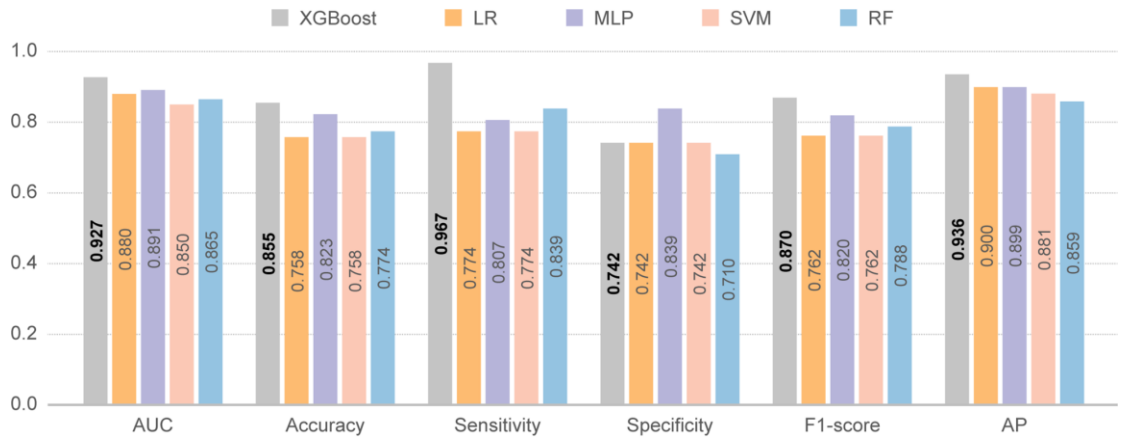

Figure S1. Performance metrics of the clinical non-imaging model, related to Figure 1.

Five machine learning models were compared to assess their performance in diagnosing VCI. Evaluation was conducted by calculating multiple metrics, including accuracy, sensitivity, specificity, F1 score, AUC, and AP. XGBoost, eXtreme gradient boosting; LR, logistic regression; MLP, multi-layer perceptron; SVM, support vector machine; RF, random forest; AUC, area under the receiver operating characteristic curve; AP, area under the precision-recall curve; VCI, vascular cognitive impairment.

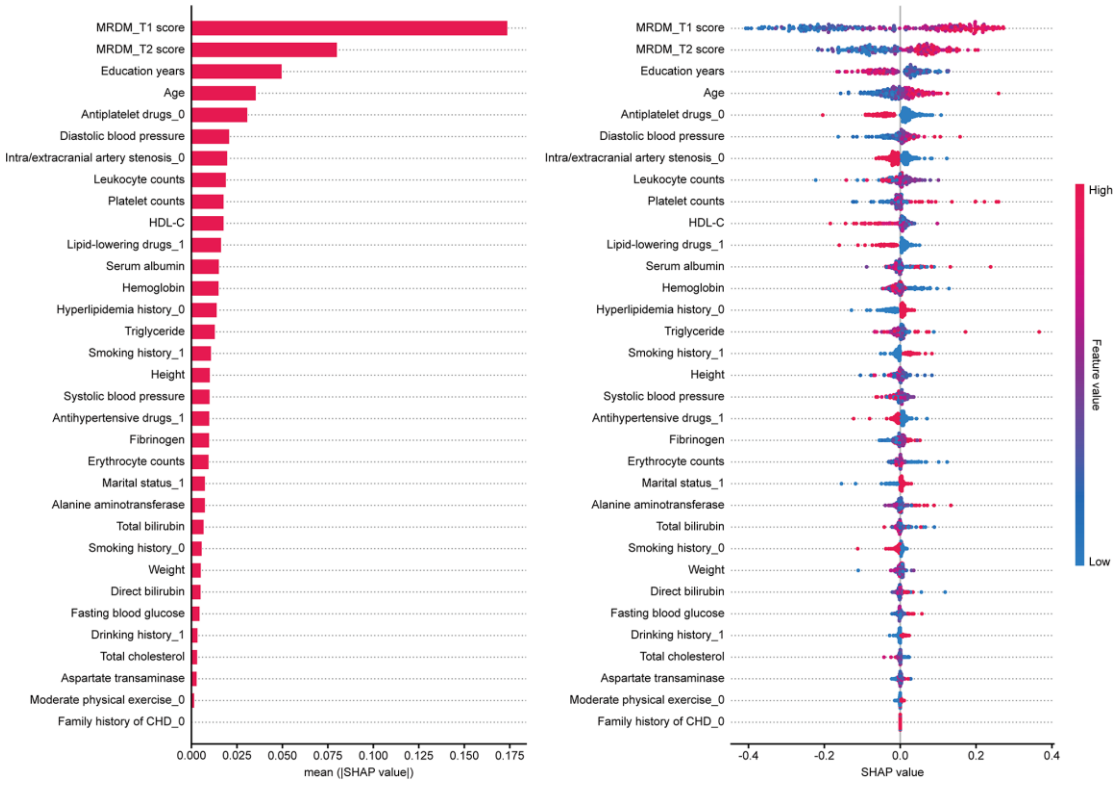

Figure S2. **SHAP analysis of the hybrid model, related to Figure 2.**

SHAP analysis was utilized to rank the contribution of thirty-three imaging and non-imaging features in the hybrid model to the diagnosis of VCI. The left plot demonstrates the mean absolute SHAP values, and the right plot illustrates the distribution of SHAP values. All features are sorted in descending order of the mean absolute SHAP values. HDL-C, high density lipoprotein cholesterol; LDL-C, low density lipoprotein cholesterol; CHD, coronary heart disease; SHAP, Shapley Additive exPlanations; sMRI, structural magnetic resonance imaging; VCI, vascular cognitive impairment.

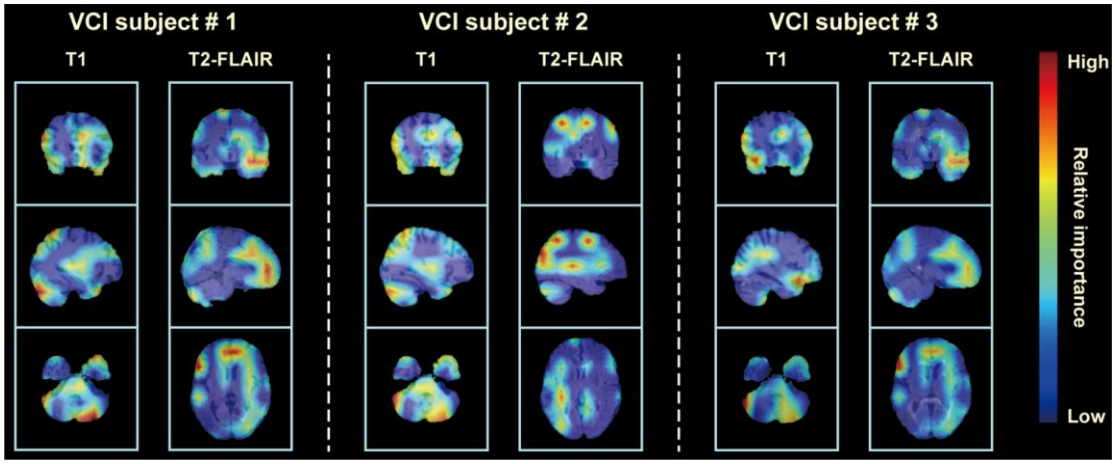

Figure S3. CAMs for three test VCI subjects generated by ViT, related to Figure 3.

CAMs of three test subjects generated by the ViT model highlighted high-risk brain regions that were associated with VCI, when T1 and T2-FLAIR images were inputted to the model, respectively. Red color indicates the brain region has a comparatively greater contribution to the VCI diagnosis in one test subject, while blue indicates a comparatively lower to the VCI diagnosis. VCI, vascular cognitive impairment; CAMs, class activation maps; ViT, Vision Transformer; FLAIR, fluid attenuated inversion recovery.

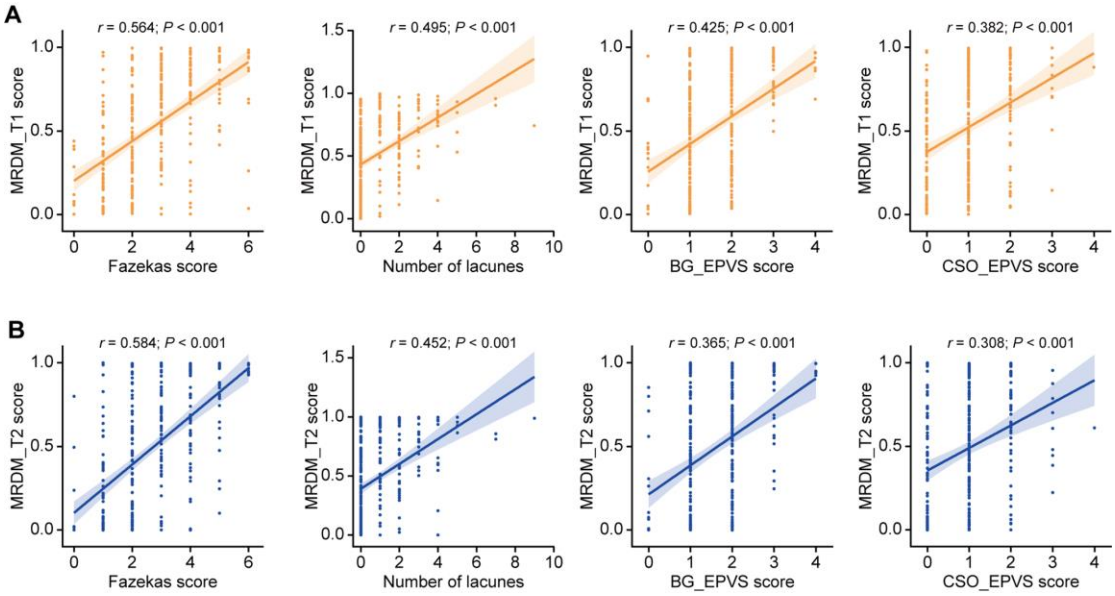

Figure S4. Association between sMRI-derived features and the neuroimaging markers of SVD, related to Figure 1.

The association between four neuroimaging markers of SVD and MRDM-T1 scores (**A**) as well as MRDM-T2 scores (**B**) was analyzed using the Spearman rank correlation test, respectively. The diagonal line represents the fitted line, and the shaded area indicates the 95% confidence interval. BG, basal ganglia; EPVS, enlarged perivascular space; CSO, centrum semiovale; sMRI, structural magnetic resonance imaging; SVD, cerebral small vessel disease.

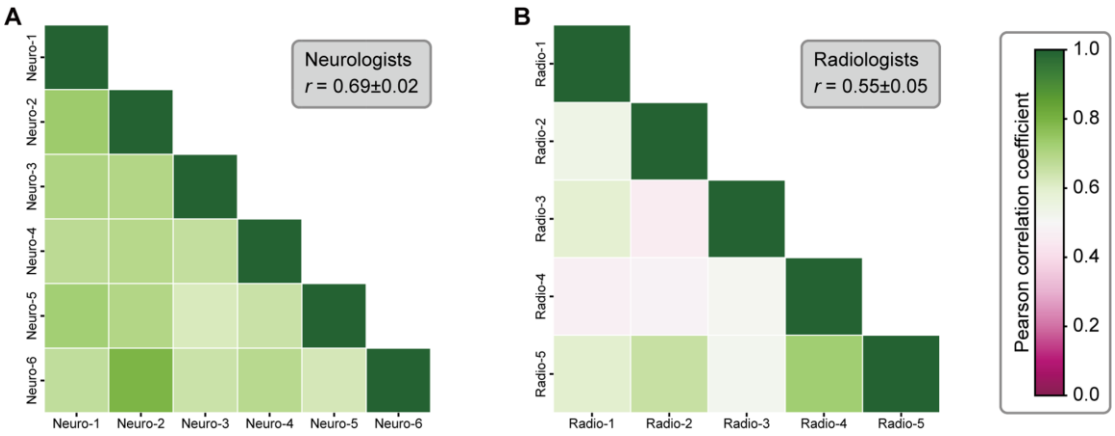

Figure S5. Inter-rater agreement among clinicians, related to Figure 6.

This figure separately displays the inter-rater agreement among neurologists (**A**) and radiologists (**B**), evaluated by calculating the pairwise Pearson correlation coefficients of their confidence scores for the VCI diagnosis. The matrices reflect the correlation coefficient values between individual neurologists and radiologists. The color gradient from magenta to green indicates increasing correlation coefficient values, suggesting higher agreement among clinicians' assessments. Furthermore, the average pairwise Pearson correlation coefficient with a 95% confidence interval is shown to represent the overall agreement within each matrix. VCI, vascular cognitive impairment.

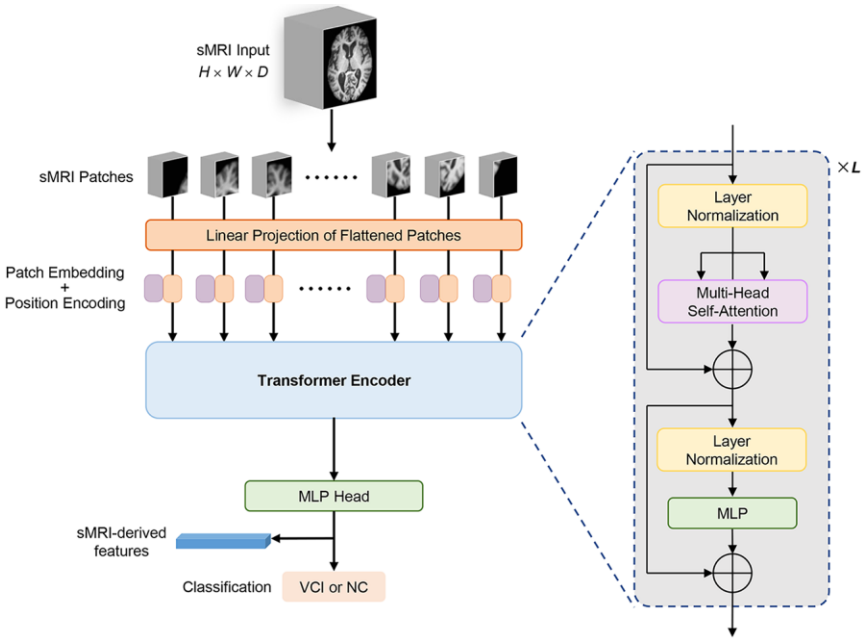

Figure S6. Architecture of the ViT backbone, related to STAR Methods.

3D images of sMRI served as input, where *H*, *W*, *D* represent the height, width, and depth of the input images, respectively. All images were split into the identical patches, and the dimensions of patches were reduced by linear projection layer. The features of all patches were combined with positional encoding, and these features with spatial information were subsequently input to the Transformer encoder to generate the deep features of networks. Ultimately, the deep features outputted from the Transformer encoder underwent processing by the MLP layer to complete the classification of VCI and NC. Furthermore, the ViT model generated the sMRI-derived features. MLP, Multi-Layer Perceptron; sMRI, structural magnetic resonance imaging; VCI, vascular cognitive impairment; NC, normal cognition; ViT, Vision Transformer.